

# Development and validation of a full physiologically-based pharmacokinetic model for sublingual buprenorphine that accounts for nonlinear bioavailability

Matthijs van Hoogdalem<sup>1</sup>, Trevor Johnson<sup>2</sup>, Alexander Vinks<sup>1</sup>, and Tomoyuki Mizuno<sup>1</sup>

<sup>1</sup>Cincinnati Children's Hospital Medical Center

<sup>2</sup>Simcyp Limited

July 20, 2022

## Abstract

Sublingual buprenorphine is used in the treatment of opioid use disorder (OUD) and neonatal opioid withdrawal syndrome (NOWS). The aim of this study was to develop a full physiologically-based pharmacokinetic (PBPK) model that can adequately describe dose- and formulation-dependent bioavailability of buprenorphine. Simcyp (v21.0) was used for model construction. Linear regression modeling was explored to describe sublingual absorption of buprenorphine across dose. Published clinical trial data not used in model development were used for validation. The PBPK model's predictive performance was deemed adequate if the geometric means of ratios between predicted and observed (P/O ratios) area under the curve (AUC), apparent clearance (CL/F), peak concentration ( $C_{\max}$ ), and time to reach  $C_{\max}$  ( $T_{\max}$ ) fell within the 1.25-fold prediction error range. Sublingual buprenorphine absorption was best described by a regression model with logarithmically transformed dose. By integrating this nonlinear absorption profile, the PBPK model adequately predicted buprenorphine pharmacokinetics (PK) following administration of sublingual tablets and solution across a dose range of 2–32 mg, with geometric mean (95% confidence interval) P/O ratios for AUC, CL/F,  $C_{\max}$ , and  $T_{\max}$  equaling 0.99 (0.86–1.12), 1.04 (0.92–1.18), 1.24 (1.09–1.40), and 1.07 (0.95–1.20), respectively. In conclusion, a fully validated PBPK model was developed that adequately predicts dose- and formulation-dependent buprenorphine PK following sublingual administration. The model forms the foundation on which a fetomaternal PBPK model for buprenorphine can be built. Fetomaternal PBPK modeling will allow conceptualization of prenatal buprenorphine exposure and investigation of its influence on postnatal NOWS severity.

## INTRODUCTION

The opioid epidemic continues to worsen and expand across the United States. Synthetic opioids, especially illicitly manufactured fentanyl, are now the leading cause of drug overdose deaths. Between 2013 and 2019, the synthetic opioid-involved death rate increased more than 10-fold, from 1.0 to 11.4 per 100,000 [1]. Buprenorphine, administered as a sublingual tablet or solution, is used in the management of opioid use disorder (OUD). Buprenorphine acts as a partial agonist at the  $\mu$  opioid receptor [2], as an antagonist at  $\delta$  and  $\kappa$  opioid receptors [3, 4], and as a full agonist at the nociceptin/orphanin FQ (NOP) opioid receptor [5]. This intricate pharmacological profile gives rise to buprenorphine's more desirable clinical properties compared to other opioids, such as lower abuse potential and reduced likelihood of fatal respiratory depression [6]. Among Medicaid enrollees diagnosed with OUD, the use of buprenorphine increased from 28.1% to 37.3% between 2014 and 2018, making it the most prescribed medication to treat OUD [7].

Opioid use during pregnancy is not uncommon. In 2019, 6.6% of pregnant women self-reported use of prescription opioids, of which 21.2% disclosed opioid misuse [8]. Newborns prenatally exposed to opioids are at risk of developing neonatal opioid withdrawal syndrome (NOWS) after birth. NOWS is characterized by gastrointestinal dysfunction and neurologic excitability [9], and requires pharmacological treatment

in those neonates whose symptoms are otherwise insufficiently controlled [10]. Sublingually administered buprenorphine is an emerging treatment for NOWS [11], but current dosing strategies have been empirically established and lack a robust pharmacokinetic (PK) and pharmacodynamic (PD) rationale. Neonatal buprenorphine PK is highly variable [12-14], and recent physiologically-based pharmacokinetic (PBPK) modeling and simulation by our group indicated variability is likely driven by differences in the extent of sublingual absorption, biliary clearance, and cytochrome P450 (CYP) 3A4 activity, especially early in life [15]. Strategies to improve the treatment of NOWS with buprenorphine include further improving our understanding of the complex PK/PD relationship and subsequently adjusting the starting dose to the expected PK profile of the neonate. Additionally, initial dosing could be tailored to the anticipated NOWS severity.

The severity of NOWS differs greatly between affected neonates, but symptoms tend to be more severe in newborns born at term [16], whose mothers used tobacco during pregnancy [17, 18], and those who had greater opioid exposure *in utero* [19]. Estimating the extent of prenatal opioid exposure is challenging. Intuitively, fetal opioid exposure may strongly correlate with maternal intake, but studies have failed to demonstrate a consistent relationship between maternal OUD medication dose and postnatal NOWS severity [17, 20-22]. This may be, in part, explained by the everchanging nature of maternal opioid PK during pregnancy and the likelihood that fetuses are more vulnerable to opioid effects at certain points during gestation [19]. Fetomaternal PBPK modeling offers a comprehensive framework that can incorporate the kaleidoscopic interplay of maternal and fetal factors that ultimately dictate prenatal opioid exposure. This, in turn, can open the way for precision treatment of NOWS based on the prenatally modeled severity.

Accurately predicting buprenorphine PK following sublingual administration is challenging since bioavailability is dependent on the formulation (tablet *vs.* solution) [23-27] and decreases with dose [26, 28, 29]. Several PBPK models for sublingual buprenorphine have been developed to date, but none have adequately integrated nonlinear bioavailability. Kalluri et al. [30] constructed a full PBPK model, which was later expanded to a pregnancy PBPK model [31], but others were not able to recreate these models due to the ambiguous description of sublingual absorption [32]. Our group developed a neonatal minimal PBPK model [15], which was based on a model developed by Johnson et al. [33], but given the neonatal application, the model was only validated for low doses, and does not accurately capture reduced bioavailability with higher doses. To lay a strong foundation for planned fetomaternal PBPK modeling, the aim of the present study was to develop a full PBPK model for buprenorphine that can adequately describe dose- and formulation-dependent bioavailability following sublingual administration.

## MATERIALS AND METHODS

### *PBPK model development*

A full PBPK model for buprenorphine was constructed and validated using Simcyp (v21.0; Simcyp Limited, Sheffield, UK). A schematic representation of the PBPK model is shown in **Figure 1**. Drug physiochemical and physiological parameters used to build the PBPK model are shown in **Table 1** [33-45].

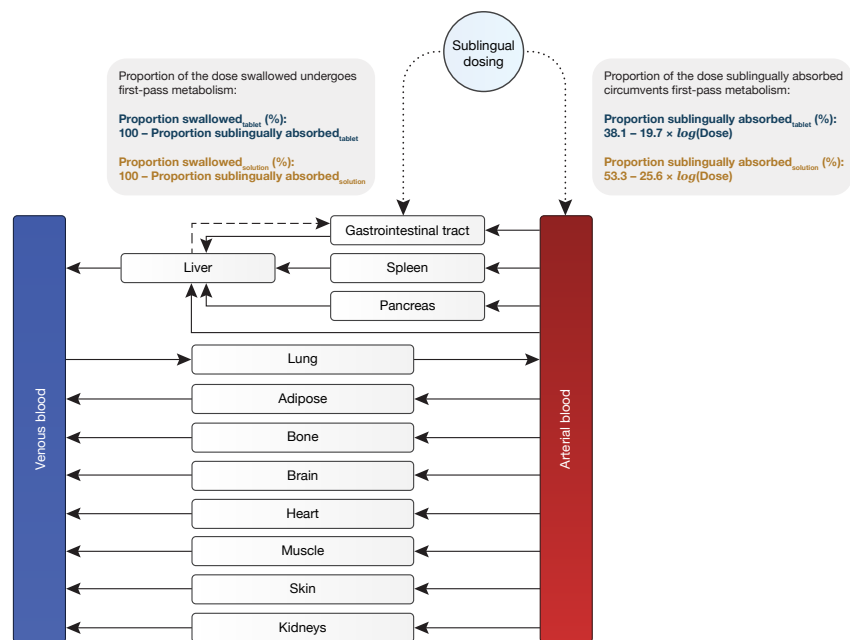


Figure 1: Full physiologically-based pharmacokinetic (PBPK) model structure. The sublingual route of administration is not available in Simcyp; sublingual absorption is therefore mimicked by employing the first-order inhalation model in combination with the inhaled route of administration. The proportion of the dose inhaled equals the proportion sublingually absorbed. The remaining fraction of the dose is swallowed.

Table 1. Input data for the full physiologically-based pharmacokinetic (PBPK) model for buprenorphine

Parameter	Value	Reference
Physiochemical		
Molecular weight (g/mol)	467.6	NCBI [34]
Log $P$	4.98	Avdeef et al. [35]
Compound type	Ampholyte	Avdeef et al. [35]
pK <sub>a</sub> (acid; phenol)	9.62	Avdeef et al. [35]
pK <sub>a</sub> (base; amine)	8.31	Avdeef et al. [35]
Blood binding		
B/P	1	Bullingham et al. [36]
f <sub>u, plasma</sub>	0.04	Elkader and Sproule [37]
Plasma binding components	AGP	Takahashi et al. [38]
Gastrointestinal tract absorption (first-order model)		
f <sub>a</sub>	1 <sup>a</sup>	
k <sub>a</sub> (h <sup>-1</sup> )	0.02 <sup>b</sup>	
Lag time (h)	0.22 <sup>c</sup>	
f <sub>u, gut</sub>	0.4 <sup>b</sup>	
Q <sub>gut</sub> (L/h)	16.8 <sup>d</sup>	
P <sub>eff, man</sub> (10 <sup>-4</sup> cm/s)	6.83 <sup>d</sup>	
Caco-2 7.4:7.4 (10 <sup>-6</sup> cm/s)	66.7	Hasan et al. [39]
Lung <sup>e</sup> absorption (first-order model)		
f <sub>a</sub>	1 <sup>a</sup>	
k <sub>a</sub> (h <sup>-1</sup> )	1 <sup>b</sup>	
Proportion of dose inhaled <sup>e</sup> <sub>tablet</sub> (%)	38.1 – 19.7 × log(Dose) <sup>f</sup>	
Proportion of dose inhaled <sup>e</sup> <sub>solution</sub> (%)	53.3 – 25.6 × log(Dose) <sup>f</sup>	
Distribution (full PBPK model)		
Tissue-to-		

The present model was based on a minimal PBPK model for buprenorphine developed earlier by our group [15], which, in turn, was adapted from a model described by Johnson et al. [33]. The minimal PBPK model was expanded to a full PBPK model by incorporating tissue-to-plasma partition coefficients ( $K_p$ ).  $K_p$  values were estimated using tissue distribution data in rats generally measured between 1 and 144 hours following subcutaneous injection of radiolabeled buprenorphine [38, 40]. Moment-dependent distribution of buprenorphine and its metabolites was considered when determining optimal time points to calculate  $K_p$  values, *e.g.*,  $K_p$  values for gut, kidney, and liver were obtained using distribution data measured at 1 hour postdose to minimize measuring the distribution of buprenorphine metabolites rather than buprenorphine.

Following expansion to a full PBPK model, first-order absorption models were optimized using buprenorphine concentration-time profiles reported by Dong et al. [28] to describe sublingual absorption of buprenorphine. As the sublingual route of administration is not available in Simcyp, sublingual absorption was mimicked by employing the first-order inhalation model in combination with the inhaled route of administration as described previously [15]. In this inhalation model, the proportion of the dose inhaled equals the proportion sublingually absorbed. The remaining fraction is swallowed.

#### *Linear regression modeling of sublingual absorption*

Concentration-time data were extracted from dose-escalation [23, 26] and dose-linearity [28] studies (training data) using WebPlotDigitizer (v4.5, Ankit Rohatgi, Pacifica, CA). Area under the curve (AUC; *i.e.*,  $AUC_{0-[\tau]}$  and  $AUC_{0-\tau}$  for single and multiple dose studies, respectively) and peak concentration ( $C_{max}$ ) following sublingual tablet or solution administration were determined through Bayesian estimation by fitting the buprenorphine population PK model reported by Moore et al. [46] to these extracted concentration-time profiles using MWPharm++ (v2.0.4; Mediware Incorporated, Prague, Czech Republic). Subsequently, the proportion of the dose to be sublingually absorbed in the PBPK model to exactly recover the AUC and  $C_{max}$  observed in the clinical trial (*i.e.*, ideal proportion) was determined by reviewing PBPK model-based predicted geometric mean AUC and  $C_{max}$  under various degrees of sublingual absorption. The relationship between AUC- and  $C_{max}$ -optimized ideal proportion and dose was explored for sublingual tablets and solution separately through linear regression modeling using the stats package (v4.1.2, R Core Team) for R (v4.1.2, R Foundation for Statistical Computing, Vienna, Austria). The following bivariate linear model was used (Equation 1):

$$1) \quad \text{Proportion}_i = \alpha + \beta \times \text{Dose}$$

where  $\text{Proportion}_i$  is the AUC- or  $C_{max}$ -optimized ideal proportion (%) for clinical study  $i$ ,  $\alpha$  is the intercept,  $\beta$  is the slope, and Dose is the sublingual tablet or solution dose in milligrams. Visual inspection of the data indicated a linear or inverse exponential relationship between ideal proportion and dose. Therefore, four varieties of the linear model were explored, *i.e.*, either untransformed or with Dose,  $\text{Proportion}_i$ , or both logarithmically transformed using a decimal logarithm of base 10. Thus, in total, 16 linear regression analyses were performed, namely, four linear model varieties explaining four individual relationships (*i.e.*, AUC- and  $C_{max}$ -optimized ideal proportions *vs.* sublingual tablet and solution doses). The linear model achieving the highest mean coefficient of determination ( $R^2$ ) across the four individual relationships was selected. AUC- and  $C_{max}$ -optimized linear models were subsequently averaged, thereby obtaining two final linear models (one for sublingual tablets and one for sublingual solution) describing the relationship between ideal proportion and dose.

#### *PBPK model validation and evaluation*

Following an extensive literature search for buprenorphine PK data in healthy volunteers, the PBPK model's predictive performance was assessed for intravenous and sublingual administration successively by determining the ratio between predicted and observed (P/O ratio) AUC, clearance (CL) or apparent clearance (CL/F),  $C_{max}$ , and, in case of sublingual administration, time to reach  $C_{max}$  ( $T_{max}$ ). All data used for model validation were independent (test data), *i.e.*, not used in the development of the PBPK or sublingual absorption model.

Predicted PK parameters were obtained by running virtual trials in Simcyp and represented the geometric mean of the virtual trial’s population. The population’s age (preferably age range, but mean age if no range was reported), proportion of females (50% was assumed for studies that did not report the participants’ sex), and administered buprenorphine dose and formulation were matched to that in the clinical study. For virtual trials in which buprenorphine was sublingually administered, a coefficient of variation (CV) of 33.9% was applied to the administered dose to reflect variability in bioavailability, which is consistent with the average variation observed by Bullingham et al. [47]. The virtual cohort consisted of 100 individuals (10 individuals  $\times$  10 trials) for each simulation. The virtual trial duration was set to the time associated with the last reported observable concentration in the clinical study.

For clinical studies in which buprenorphine was intravenously administered, observed PK parameters were defined as those reported in the trial; missing values were calculated through noncompartmental analysis using Edsim++ (v2.0.4; Mediware Incorporated, Prague, Czech Republic). Clinical studies rarely determined a true  $C_{\max}$  following intravenous administration. Instead,  $C_{\max}$  generally represented the first concentration ( $C_{\text{first}}$ ) measured few minutes after completion of a bolus injection ( $T_{\text{first}}$ ). Therefore, to match predicted and observed  $C_{\max}$ , predicted  $C_{\max}$  was defined as the modeled concentration at  $T_{\text{first}}$ .

For clinical studies in which buprenorphine was sublingually administered, observed PK parameters were, similarly to described for linear regression modeling, obtained through Bayesian estimation by fitting the buprenorphine population PK model reported by Moore et al. [46] to concentration-time data extracted from publications using WebPlotDigitizer. Reported PK parameter values were not used, as some studies employed limited sampling strategies, which limited the robustness of time-associated (*i.e.*,  $T_{\max}$  and  $C_{\max}$ ) and exposure-dictated (*i.e.*, AUC and CL/F) PK parameters. In the interest of consistency, all concentration-time profiles of sublingually administered buprenorphine for each clinical study were digitized and used to estimate PK parameters through Bayesian estimation.

Potential bias in the PBPK model’s prediction following sublingual administration was evaluated using predicted *vs.* observed AUC, CL/F,  $C_{\max}$ , and  $T_{\max}$  and dose *vs.* respective P/O ratio goodness-of-fit plots.

### Statistical analysis

Geometric means and 95% confidence intervals (CIs) of PK parameter P/O ratios were calculated using the DescTools package (v0.99.44, Signorell *et mult. al.*) for R. Normal distribution of P/O ratios was examined through the Shapiro-Wilk test. The predictive performance of the PBPK model was deemed adequate if the geometric means of PK parameter P/O ratios fell between 0.8-fold and 1.25-fold (1.25-fold prediction error range). In addition to assessing whether geometric mean PK parameter P/O ratio fell within the relatively narrow 1.25-fold prediction error range, the proportion of all PK parameter P/O ratios falling within the wider 2-fold prediction error range was determined.

## RESULTS

### Validation of the PBPK model’s predictive performance following intravenous administration

The structure of the full PBPK model was first externally validated by determining P/O ratios of  $AUC_{0-[\tau]}$ , CL, and  $C_{\max}$  following intravenous administration of buprenorphine in healthy volunteers. Twelve PK studies, spanning a dose range of 0.3–16 mg and including a total of 69 subjects (aged 20 to 66.8 years) with 89 concentration-time profiles, were used for intravenous model validation (**Table 2**) [41, 47–51]. For all 12 PK studies, the P/O ratios of  $AUC_{0-[\tau]}$ , CL, and  $C_{\max}$ , fell within the 2-fold prediction error range. Geometric mean (95% CI)  $AUC_{0-[\tau]}$ , CL, and  $C_{\max}$  P/O ratios were 1.01 (0.90–1.13), 0.95 (0.84–1.08), and 0.91 (0.78–1.05), respectively, indicating adequate predictive performance of these PK parameters following intravenous administration across a wide dose range in healthy volunteers. All predicted *vs.* observed buprenorphine concentration-time profiles following intravenous administration are shown in **Figure 2**.

Table 2. Predicted and observed pharmacokinetic parameters of buprenorphine following intravenous (i.v.) administration

Clinical trial	Dose (mg)	Route of administration	n	Female (%)	Mean age [range] (years)		AUC <sub>0-∞</sub> (ng×h/mL)	CL (mL/min)	C <sub>max</sub> (ng/mL)
Bullingham et al. [47]	0.3	i.v. (1 min)	5	60	66.8	Predicted	5.96	50.3	1.39
						Observed	5.8 <sup>a</sup>	51.8 <sup>b</sup>	0.96
Bullingham et al. [47]	0.3	i.v. (1 min)	5	60	64.2	Predicted	4.76	63	1.39
						Observed	3.14 <sup>a</sup>	95.7 <sup>b</sup>	1.08
Bullingham et al. [47]	0.3	i.v. (1 min)	5	60	66	Predicted	4.65	64.4	1.38
						Observed	3.2 <sup>a</sup>	93.8 <sup>b</sup>	0.95
Bai et al. [48]	0.3	i.v. (2 min)	24	24	35.5 (20–53)	Predicted	4.8	62.5	1.71
						Observed	5.2	57.7 <sup>b</sup>	2.32
Lim et al. [49]	0.3	i.v. (5 min)	14	NR	25	Predicted	4.53	66.2	1.93
						Observed	4.09	77.7	2.73
Mendelson et al. [50]	1	i.v. (30 min)	6	16.7	29 (21–38)	Predicted	15.8	63.2	13.1
						Observed	18.4	62.5	14.3
Kuhlman et al. [41]	1.2	i.v. (1 min)	5	0	34.4 (27–41)	Predicted	19.7	60.8	25.4
						Observed	19.7	60.8	25.4

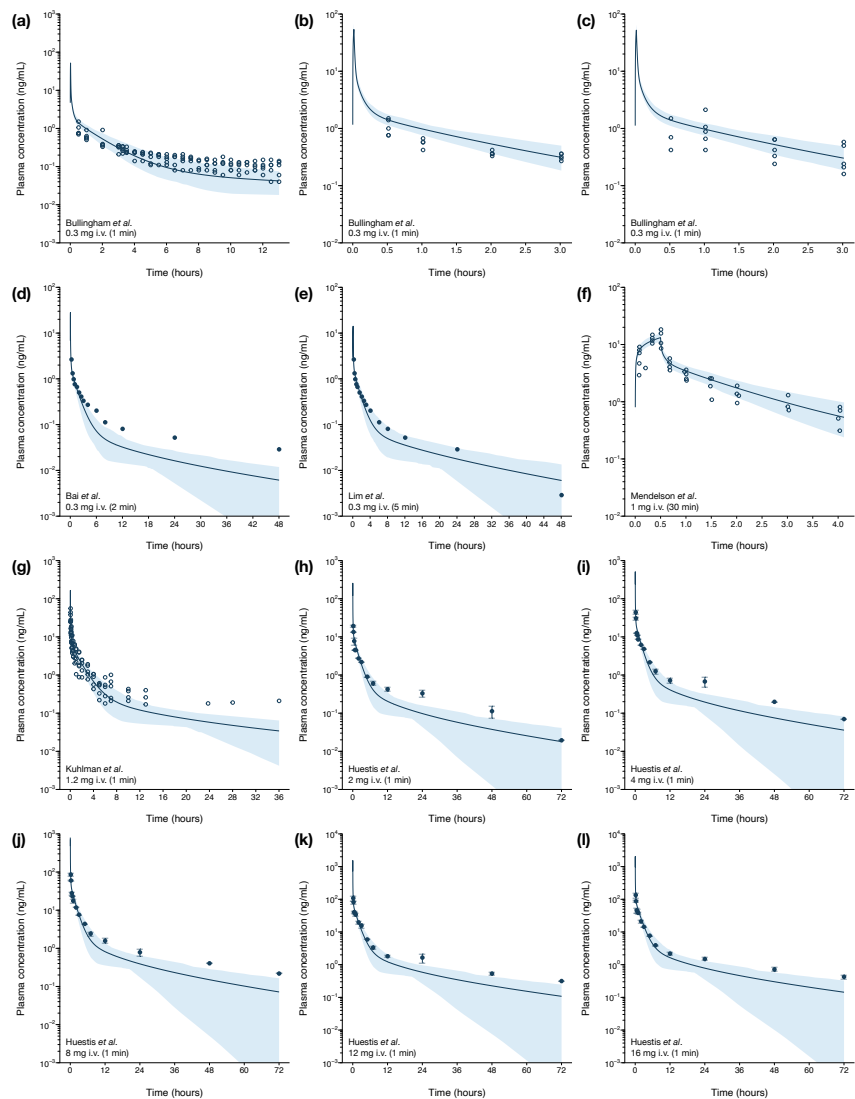


Figure 2: Physiologically-based pharmacokinetic (PBPK) model-predicted and observed concentration-time profiles of buprenorphine following intravenous (i.v.) administration. Blue solid line and shaded area represent the mean and 5th to 95th percentile range of the virtual population ( $n = 100$ ), respectively. Open circles represent individual observations. Closed circles and whiskers represent mean and standard deviation of the observations, respectively. References for reported observations are provided in **Table 2**.

### *Integrating nonlinear sublingual absorption into the PBPK model*

Linear regression models with logarithmically transformed dose best described the relationships between AUC- and  $C_{\max}$ -optimized ideal proportions and sublingual tablet and solution doses (mean  $R^2 = 0.756$ , **Figure 3**), which indicated that sublingual buprenorphine absorption is nonlinear across dose. By averaging the AUC- and  $C_{\max}$ -optimized linear regression models, two final absorption equations were obtained, namely, proportion of the dose sublingually absorbed equals  $38.1 - 19.7 \times \log(\text{Dose})$  and  $53.3 - 25.6 \times \log(\text{Dose})$  for sublingual tablets and solution, respectively. These equations were integrated into the PBPK model as shown in **Figure 1**.



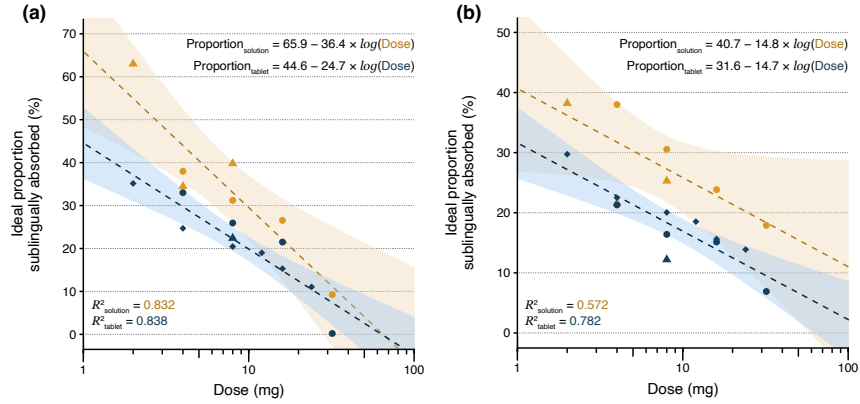


Figure 3: Proportion of the dose required by the physiologically-based pharmacokinetic (PBPK) model to be sublingually absorbed to exactly recover the (a) area under the curve (AUC; *i.e.*,  $AUC_{0-[\tau]}$  and  $AUC_{0-\tau}$  for single and multiple dose studies, respectively) and (b) peak concentration ( $C_{max}$ ) observed in the clinical trial (*i.e.*, ideal proportion) across dose. Blue and orange circles (\*), triangles ( $\Delta$ ), and diamonds ( $\diamond$ ) represent sublingual tablet and solution data obtained from Harris *et al.* [26], Schu and Johanson [23], and Dole *et al.* [27], respectively. The regression equations are shown in the upper right corners (where dose is in milligrams and logarithm base is 10), with coefficient of determination in the lower left corners. The final buprenorphine PBPK model uses the average of the AUC and  $C_{max}$  optimized equations, *i.e.*, proportions sublingually absorbed equals  $38.1 - 19.7 \log(Dose)$  and  $53.3 - 25.6 \log(Dose)$  for sublingual tablets and solution, respectively.

#### Validation and evaluation of the PBPK model's predictive performance following sublingual administration

The PBPK model with the developed description of nonlinear sublingual buprenorphine absorption was subsequently externally validated by determining P/O ratios of AUC, CL/F,  $C_{max}$ , and  $T_{max}$  following sublingual administration of buprenorphine tablets and solution separately. For validation of the PBPK model's predictive performance following sublingually administered tablets, 16 PK studies, spanning a dose range of 2–32 mg and including a total of 296 subjects (aged 19 to 54) with 419 concentration-time profiles, were used (Table 3) [25, 27, 29, 52–54]. For all 16 PK studies, the P/O ratios of AUC, CL/F,  $C_{max}$ , and  $T_{max}$  fell within the 2-fold prediction error range. Geometric mean (95% CI) AUC, CL/F,  $C_{max}$ , and  $T_{max}$  P/O ratios were 0.96 (0.82–1.12), 1.07 (0.92–1.24), 1.20 (1.05–1.37), and 1.07 (0.94–1.23), respectively.

Table 3. Predicted and observed<sup>a</sup>  
**buprenorphine pharmacokinetic  
parameters following administration of  
sublingual tablets**

Clinical trial	Dose (mg)	Route of administration	n	Fe-male (%)	Mean age [range] (years)	AUC <sup>b</sup> (ng × h/mL)	CL/FC <sub>max</sub> (ng/nL)	T <sub>max</sub> (h)	
McAleer et al. [52]	2	sublingual, tablet	27	0	(19–42)	Pre-dicted	7.32	273.11.37	1.14
						Ob-served	10.3	195.11.47	1.48
Ciraulo et al. [29]	4	sublingual, tablet	23	30.4	34.5	Pre-dicted	0.71	1.4 0.93	0.77
						Ob-served	15.9	252.22.67	1.12
Jönsson et al. [53]	4	sublingual, tablet	61	41	(19–54)	Pre-dicted	1.65	0.61 1.43	1.12
						Ob-served	13.7	291.52.31	1.08
Nath et al. [27]	8	sublingual, tablet	6	0	(23–42)	Pre-dicted	0.63	1.59 1.08	0.64
						Ob-served	22.6	353.33.52	1.15
McAleer et al. [52]	8	sublingual, tablet	27	0	(19–42)	Pre-dicted	0.96	1.04 1.19	1.05
						Ob-served	23.5	340.52.95	1.1
Ciraulo et al. [29]	8	sublingual, tablet	23	30.4	34.5	Pre-dicted	0.79	1.27 0.91	0.9
						Ob-served	22.9	350 3.49	1.14
	10					Ob-served	29.1	275.33.84	1.27
						P/O ratio	0.79	1.27 0.91	0.9
						Pre-dicted	27.1	295 4.15	1.12

For validation of the predictive performance following administration of sublingual solution, seven PK studies, spanning a dose range of 2–16 mg and including a total of 75 subjects (aged 21 to 42) with 81 concentration-time profiles, were used (**Table 4**) [25, 27, 41, 50]. For all seven PK studies, the P/O ratios of AUC, CL/F, and  $T_{\max}$  fell within the 2-fold prediction error range. The P/O ratio for  $C_{\max}$  fell within the 2-fold prediction error range in six out of seven (85.7%) PK studies. Geometric mean (95% CI) AUC, CL/F,  $C_{\max}$ , and  $T_{\max}$  P/O ratios were 1.05 (0.75–1.46), 0.98 (0.72–1.33), 1.34 (0.95–1.90), and 1.06 (0.79–1.41), respectively.

Table 4. Predicted and observed<sup>a</sup>  
**buprenorphine pharmacokinetic  
 parameters following administration  
 of sublingual solution**

Clinical trial	Dose (mg)	Route of administration	n	Fe-male (%)	Mean age [range] (years)	AUC <sup>b</sup> (ng × h/mL)	CL/FC <sub>max</sub> (ng/mL)	T <sub>max</sub> (h)		
Mendelson et al. [50]	2	sublingual, solution (3 min hold)	6	16.7	29 (21–38)	Pre-dicted	9.36	213.61.94	1.11	
						Ob-served	14.3 <sup>c</sup>	139.9 <sup>c</sup>	1.6 <sup>c</sup>	1.25 <sup>c</sup>
Mendelson et al. [50]	2	sublingual, solution (5 min hold)	6	16.7	29 (21–38)	Pre-dicted	9.36	213.61.94	1.11	
						Ob-served	13.2 <sup>c</sup>	151.5 <sup>c</sup>	1.72 <sup>c</sup>	1.62 <sup>c</sup>
Kuhlman et al. [41]	4	sublingual, solution	6	0	34.4 (27–40)	Pre-dicted	17.1	233.63.28	1.15	
						Ob-served	15	266.53.22	0.6	1.92
Nath et al. [27]	8	sublingual, solution	6	0	28 (23–42)	Pre-dicted	28.9	277	5.19	1.14
						Ob-served	34.6	230.96.72	1.02	1.12
Chawarski et al. [25]	8	sublingual, solution, m.d.	18	29.5	37.8	Pre-dicted	35	239.26.38	1.12	
						Ob-served	25.4	315.63.19	1.18	0.95

<sup>a</sup> Clinical trial data; <sup>b</sup> Predicted values; <sup>c</sup> Observed values

On average for tablet and solution formulations, the geometric mean (95% CI) AUC, CL/F,  $C_{\max}$ , and  $T_{\max}$  P/O ratios were 0.99 (0.86–1.12), 1.04 (0.92–1.18), 1.24 (1.09–1.40), and 1.07 (0.95–1.20), respectively. All predicted *vs.* observed buprenorphine concentration-time profiles following sublingual administration are shown in **Figure 4**. Predicted *vs.* observed goodness-of-fit plots for AUC, CL/F, and  $T_{\max}$  did not reveal a bias, as data points were symmetrically distributed across the line of equality (**Figure 5**). Similarly, dose *vs.* P/O ratio goodness-of-fit plots suggested an unbiased prediction of AUC, CL/F, and  $T_{\max}$  across dose (**Figure 6**), although clinical studies in which participants received sublingual solution were relatively few and the dose range was smaller. Although goodness-of-fit plots indicated a modest trend towards overpredicting  $C_{\max}$ , especially for high doses, the PBPK model’s predictive performance of buprenorphine PK following sublingual administration seemed to overall be adequate for both formulations across a wide dose range in healthy volunteers.

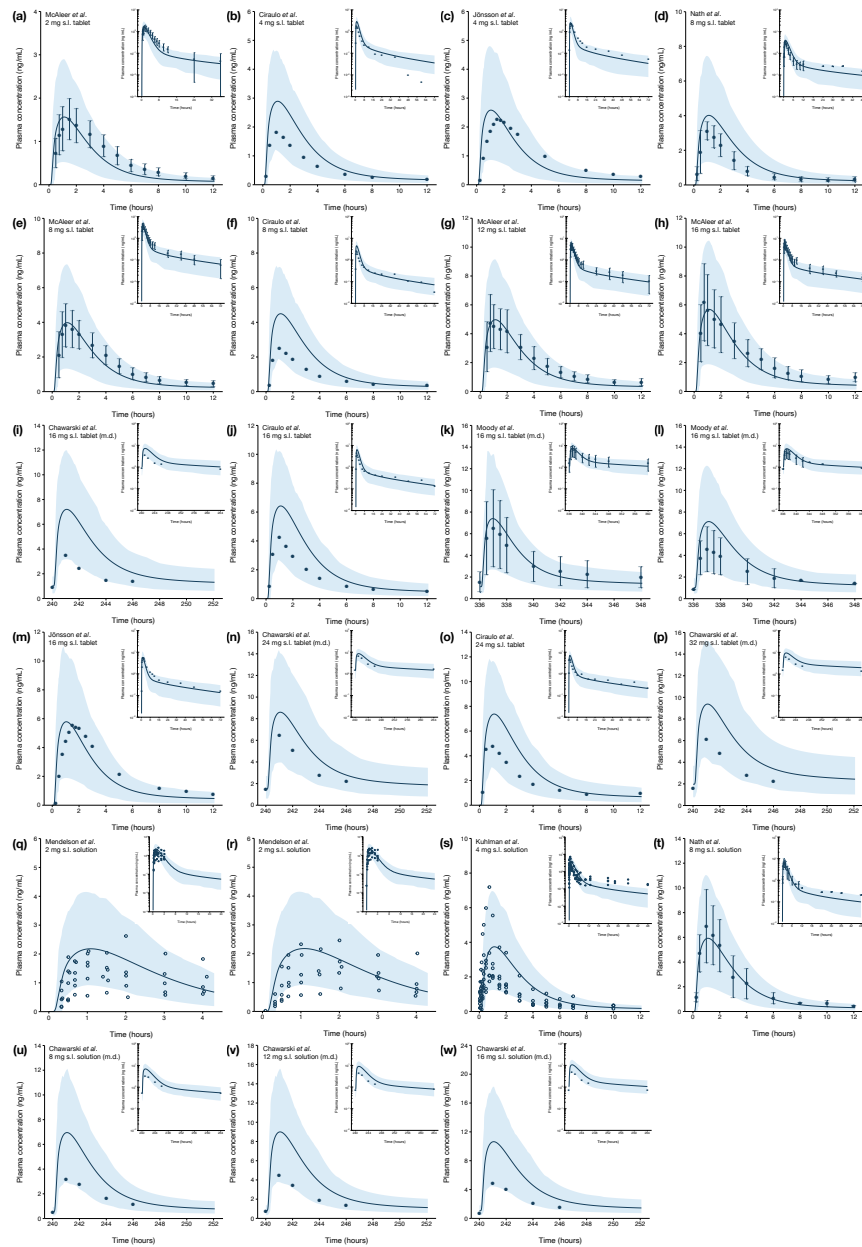


Figure 4: Physiologically-based pharmacokinetic (PBPK) model-predicted and observed concentration-time profiles of buprenorphine following sublingual (s.l.) administration. Blue solid line and shaded area represent the mean and 5th to 95th percentile range of the virtual population ( $n = 100$ ), respectively. Open circles represent individual observations. Closed circles and whiskers represent mean and standard deviation of the observations, respectively. References for reported observations are provided in **Table 3 and 4**.

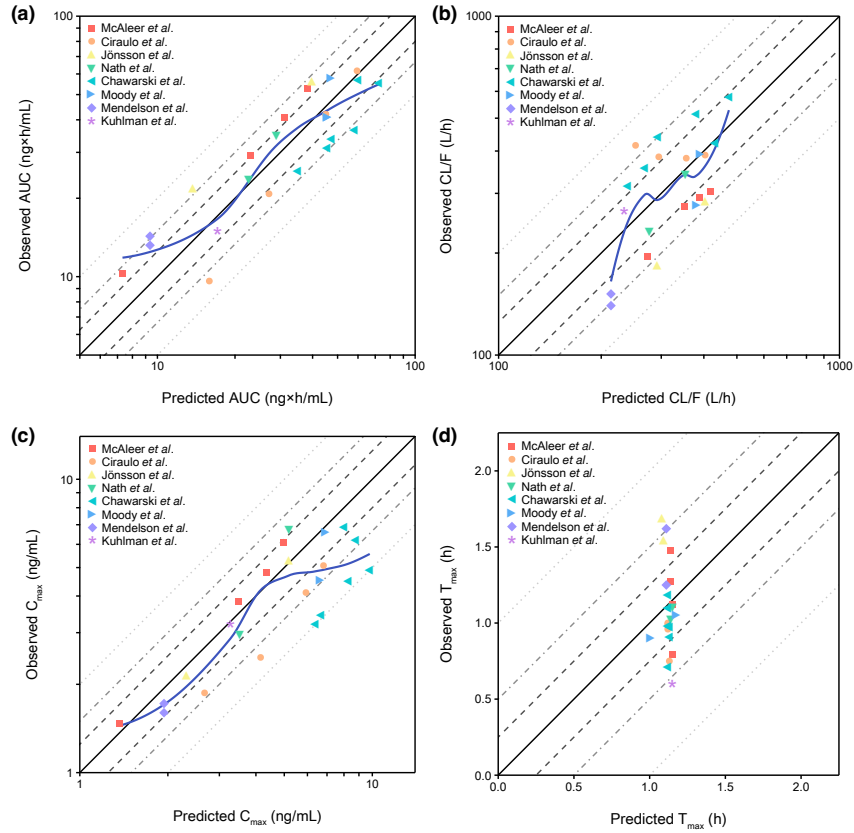


Figure 5: Goodness-of-fit plots for the final sublingual buprenorphine physiologically-based pharmacokinetic (PBPK) model, showing PBPK model-based predicted versus observed (a) area under curve (AUC; *i.e.*,  $AUC_{0-[\tau]}$  and  $AUC_{0-\tau}$  for single and multiple dose studies, respectively), (b) apparent clearance (CL/F), (c) peak concentration ( $C_{max}$ ), and (d) time to reach  $C_{max}$  ( $T_{max}$ ). In each panel, the solid black line represents the line of equality, where grayscale dashed, dot-and-dash, and dotted lines represent 1.25-, 1.5-, and 2-fold prediction error ranges, respectively. Curved blue solid lines represent locally estimated scatterplot smoothing (LOESS) curves.

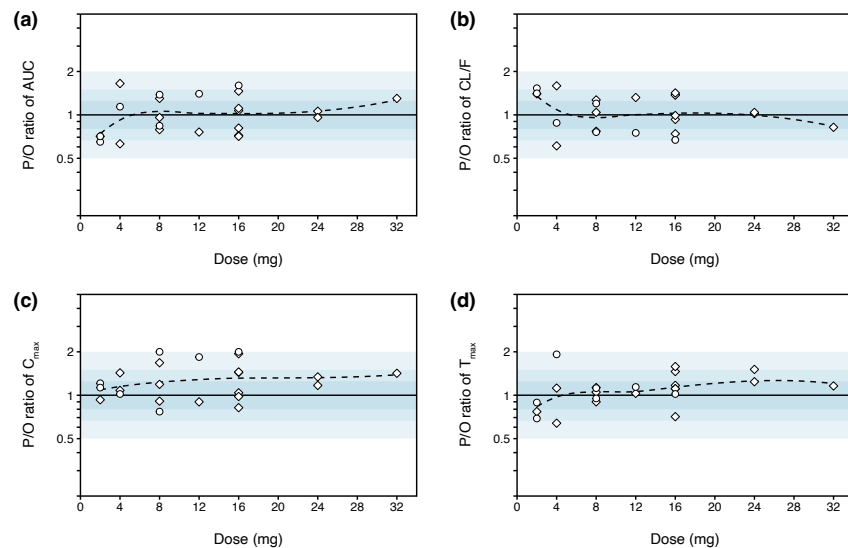


Figure 6: Goodness-of-fit plots for the final sublingual buprenorphine physiologically-based pharmacokinetic (PBPK) model, showing dose versus the ratio between predicted and observed (P/O ratio) (a) area under curve (AUC; *i.e.*,  $AUC_{0-[\tau]}$  and  $AUC_{0-\tau}$  for single and multiple dose studies, respectively), (b) apparent clearance (CL/F), (c) peak concentration ( $C_{max}$ ), and (d) time to reach  $C_{max}$  ( $T_{max}$ ), as listed in **Table 3 and 4**. Sublingual tablet and solution doses are represented by diamonds (\*) and circles (\*), respectively. In each panel, the solid black line represents the line of equality, where descending shades of blue filled areas represent 1.25-, 1.5-, and 2-fold prediction error ranges, respectively. Curved black dashed lines represent locally estimated scatterplot smoothing (LOESS) curves.

## DISCUSSION

This is the first study to describe dose- and formulation-dependent sublingual buprenorphine absorption across a wide dose range through PBPK modeling. The developed model will serve as a foundation to build a fetomaternal PBPK model for buprenorphine on, which can be used to explore the relationship between fetal buprenorphine exposure and the severity of NWS postnatally. By integrating a novel description of nonlinear sublingual buprenorphine absorption, the model adequately predicted PK following administration of sublingual tablets and solution. First, the full PBPK model structure was successfully externally validated using published intravenous PK data. Subsequently, a total of 23 published PK studies not used for model development, in which 371 healthy volunteers received buprenorphine as either sublingual tablet or solution across a dose range of 2–32 mg, were used to validate the final PBPK model. Geometric mean P/O ratios of AUC, CL/F,  $C_{max}$ , and  $T_{max}$  were close to unity and fell within the 1.25-fold prediction error range. Goodness-of-fits plots indicated unbiased prediction of all PK parameters, except for  $C_{max}$ , which suggested a moderate trend towards overprediction, especially for high doses.

Previous studies have demonstrated nonlinear PK of sublingually administered buprenorphine (either as tablet or solution) across the entire dose range used for the management of OUD [26, 28, 29]. PK following intravenous administration, in contrast, is linear [51], which strongly suggests that nonlinearity observed under sublingual dosing is driven by varying bioavailability, rather than by changes in clearance. Various mechanisms have been proposed to explain nonlinear bioavailability, including varying dissolution degrees and times between tablet strengths [26], where high-dosed formulations may need to be kept *in situ* longer to allow maximal absorption, thereby increasing the risk of swallowing relatively more of the dose. In addition, buprenorphine sequesters in oral tissues [55], which decreases the concentration gradient that drives sublingual absorption of buprenorphine. The absorption model proposed in this study captures nonlinear



bioavailability observed clinically. It is, however, important to note that the model was developed using PK data across a dose range of 2–32 mg [23, 26, 28]. We caution against applying the absorption model outside this dose interval.

The developed model has a few limitations.  $K_p$  values used to describe distribution of buprenorphine across various organs were obtained from rat data [38, 40] and may therefore not capture human physiology in all respects. More importantly, distribution in rats was not measured under strict steady-state conditions [38, 40], which limits the robustness of the  $K_p$  values estimated in this study. Nevertheless, using these  $K_p$  values, observed concentrations were well-captured by the PBPK model and the volume of distribution at steady-state ( $V_{ss}$ ) was furthermore calculated at 6.23 L/kg in Simcyp, which approximates 4.95 L/kg observed clinically [41]. We explored using the Rodgers and Rowland [56] method as an alternative to predict tissue distribution (method 2 in Simcyp), but this resulted in an estimated  $V_{ss}$  of 23.0 L/h, which would necessitate the application of an empirically identified  $K_p$  scalar to recover the observed  $V_{ss}$ . Instead, we deemed distribution estimated from rat data, albeit not measured under ideal steady-state conditions, to be more in line with the physiological rationale of PBPK modeling.

Another limitation is that the present model overestimates  $C_{max}$  modestly following sublingual administration of buprenorphine tablets and solution (geometric mean P/O ratios of 1.20 and 1.34, respectively). Manual parameter estimation of ideal proportion would preferably have yielded one and the same value to recover both observed AUC and  $C_{max}$  simultaneously for each dose, but ideal proportion values for AUC and  $C_{max}$  diverged, especially at the lower and upper limits of the dose spectrum (**Figure 3**). This indicates an oversimplification of sublingual absorption in the current PBPK model. The model accounts for differences in the total transfer of buprenorphine across oral mucosa, but the rate of this process is likely variable across dose and formulation. Absorption rate differences were not integrated into the PBPK model, and AUC- and  $C_{max}$ -optimized nonlinear absorption models were instead averaged, leading to a modest overestimation of  $C_{max}$  overall. To understand the implication of this overestimation, it is worthwhile to briefly review the PK/PD relationship of buprenorphine, and, specifically, the degree by which its PD effect is explained by  $C_{max}$  compared to AUC. Yassen et al. [57] characterized the PK/PD relationship of buprenorphine in healthy volunteers with respect to its respiratory depressant effect, which is an unambiguous marker for buprenorphine’s penetration into the central nervous system (CNS) and its receptor association/dissociation kinetics at the  $\mu$ -opioid receptor [58]. They estimated the time required for concentration at the effect site to reach 50% of the plasma concentration ( $t_{1/2,ke0}$ ) for buprenorphine at 75.3 minutes [57], which, relative to other opioids, indicates a slow onset of action, but a longer duration, where its effect is only marginally driven by  $C_{max}$  [59]. Since the developed PBPK model adequately predicts AUC following sublingual administration of buprenorphine, we believe the implications of modestly overestimating  $C_{max}$  are therefore limited.

## CONCLUSION

The full PBPK model developed in this study is the first to adequately capture buprenorphine PK following sublingual administration (either as tablet or solution) across a wide dose range. The model provides valuable insights into the mechanisms that underly complex sublingual buprenorphine PK. Potential applications of the model include using it to optimize the treatment of OUD with buprenorphine, but for our group specifically, the model forms the basis for planned fetomaternal PBPK modeling endeavors. Improving the treatment of NOWS requires tailoring of pharmacotherapy based on the expected severity of withdrawal symptoms. Fetomaternal PBPK modeling of buprenorphine facilitates estimation of prenatal buprenorphine exposure throughout gestation based on the maternal intake, which opens the way for examining the likely link it has with postnatal withdrawal severity. This, in turn, could enable fetomaternal PBPK model-informed precision dosing of buprenorphine, which is expected to improve the clinical outcomes of neonates affected by NOWS. The thoroughly validated PBPK model for buprenorphine developed in this study forms the fundament for this task.

## ACKNOWLEDGMENTS

The graphical abstract of this manuscript was partly created with BioRender.com.

## FUNDING

The project described was supported in part by the National Center for Advancing Translational Sciences of the National Institutes of Health (NIH), under Award Number 2UL1TR001425-05A1, and the Maternal and Pediatric Precision in Therapeutics (MPRINT) Knowledge & Research Coordination Center (KRCC) of the Eunice Kennedy Shriver National Institute of Child Health and Human Development (NICHD), under Award Number 1P30HD106451. The content is solely the responsibility of the authors and does not necessarily represent the official views of the NIH and the NICHD. M.W.v.H. was supported by the Rieveschl/Parke-Davis Doctoral Candidacy Scholarship of the University of Cincinnati.

## CONFLICT OF INTEREST

T.N.J. is an employee of Certara UK Limited, Simcyp Division. All other authors declared no competing interests for this work.

## AUTHOR CONTRIBUTION

M.W.v.H. wrote the manuscript. M.W.v.H., A.A.V., and T.M. designed the research, M.W.v.H., T.N.J., and T.M. performed the research, and M.W.v.H., T.N.J., A.A.V., and T.M. analyzed the data.

## REFERENCES

1. Mattson CL, Tanz LJ, Quinn K, Kariisa M, Patel P, Davis NL. Trends and geographic patterns in drug and synthetic opioid overdose deaths - United States, 2013-2019. *MMWR Morb Mortal Wkly Rep.* 2021;70:202-7. <https://doi.org/10.15585/mmwr.mm7006a4>.
2. Martin WR, Eades CG, Thompson JA, Huppler RE, Gilbert PE. The effects of morphine- and nalorphine- like drugs in the nondependent and morphine-dependent chronic spinal dog. *J Pharmacol Exp Ther.* 1976;197:517-32.
3. Negus SS, Bidlack JM, Mello NK, Furness MS, Rice KC, Brandt MR. Delta opioid antagonist effects of buprenorphine in rhesus monkeys. *Behav Pharmacol.* 2002;13:557-70. <https://doi.org/10.1097/00008877-200211000-00005>.
4. Leander JD. Buprenorphine is a potent kappa-opioid receptor antagonist in pigeons and mice. *Eur J Pharmacol.* 1988;151:457-61. [https://doi.org/10.1016/0014-2999\(88\)90543-2](https://doi.org/10.1016/0014-2999(88)90543-2).
5. Wnendt S, Krüger T, Janocha E, Hildebrandt D, Englberger W. Agonistic effect of buprenorphine in a nociceptin/OFQ receptor-triggered reporter gene assay. *Mol Pharmacol.* 1999;56:334-8. <https://doi.org/10.1124/mol.56.2.334>.
6. Pergolizzi J, Aloisi AM, Dahan A, Filitz J, Langford R, Likar R, et al. Current knowledge of buprenorphine and its unique pharmacological profile. *Pain Pract.* 2010;10:428-50. <https://doi.org/10.1111/j.1533-2500.2010.00378.x>.
7. Donohue JM, Jarlenski MP, Kim JY, Tang L, Ahrens K, Allen L, et al. Use of medications for treatment of opioid use disorder among US Medicaid enrollees in 11 states, 2014-2018. *JAMA.* 2021;326:154-64. <https://doi.org/10.1001/jama.2021.7374>.
8. Ko JY, D'Angelo DV, Haight SC, Morrow B, Cox S, Salvesen von Essen B, et al. Vital signs: prescription opioid pain reliever use during pregnancy — 34 U.S. jurisdictions, 2019. *MMWR Morb Mortal Wkly Rep.* 2020;69:897–903. <https://doi.org/10.15585/mmwr.mm6928a1>.
9. Hudak ML, Tan RC. Neonatal drug withdrawal. *Pediatrics.* 2012;129:e540-60. <https://doi.org/10.1542/peds.2011-3212>.
10. Wachman EM, Schiff DM, Silverstein M. Neonatal abstinence syndrome: advances in diagnosis and treatment. *JAMA.* 2018;319:1362-74. <https://doi.org/10.1001/jama.2018.2640>.

11. Simon AE, Freund MP, Archer SW, Bremer AA. Toward the use of buprenorphine in infants for neonatal opioid withdrawal syndrome: summary of an NIH workshop. *J Perinatol*. 2021;1-3. <https://doi.org/10.1038/s41372-020-00886-7>.
12. Ng CM, Dombrowsky E, Lin H, Erlich ME, Moody DE, Barrett JS, et al. Population pharmacokinetic model of sublingual buprenorphine in neonatal abstinence syndrome. *Pharmacotherapy*. 2015;35:670-80. <https://doi.org/10.1002/phar.1610>.
13. Mizuno T, McPhail BT, Kamatkar S, Wexelblatt S, Ward L, Christians U, et al. Physiologic indirect response modeling to describe buprenorphine pharmacodynamics in newborns treated for neonatal opioid withdrawal syndrome. *Clin Pharmacokinet*. 2021;60:249-59. <https://doi.org/10.1007/s40262-020-00939-2>.
14. van Hoogdalem MW, McPhail BT, Hahn D, Wexelblatt SL, Akinbi HT, Vinks AA, et al. Pharmacotherapy of neonatal opioid withdrawal syndrome: a review of pharmacokinetics and pharmacodynamics. *Expert Opin Drug Metab Toxicol*. 2021;17:87-103. <https://doi.org/10.1080/17425255.2021.1837112>.
15. van Hoogdalem MW, Johnson TN, McPhail BT, Kamatkar S, Wexelblatt SL, Ward LP, et al. Physiologically-based pharmacokinetic modeling to investigate the effect of maturation on buprenorphine pharmacokinetics in newborns with neonatal opioid withdrawal syndrome. *Clin Pharmacol Ther*. 2022;111:496-508. <https://doi.org/10.1002/cpt.2458>.
16. Liu AJ, Jones MP, Murray H, Cook CM, Nanan R. Perinatal risk factors for the neonatal abstinence syndrome in infants born to women on methadone maintenance therapy. *Aust N Z J Obstet Gynaecol*. 2010;50:253-8. <https://doi.org/10.1111/j.1479-828X.2010.01168.x>.
17. Bakstad B, Sarfi M, Welle-Strand GK, Ravndal E. Opioid maintenance treatment during pregnancy: occurrence and severity of neonatal abstinence syndrome. A national prospective study. *Eur Addict Res*. 2009;15:128-34. <https://doi.org/10.1159/000210042>.
18. Choo RE, Huestis MA, Schroeder JR, Shin AS, Jones HE. Neonatal abstinence syndrome in methadone-exposed infants is altered by level of prenatal tobacco exposure. *Drug Alcohol Depend*. 2004;75:253-60. <https://doi.org/10.1016/j.drugalcdep.2004.03.012>.
19. van Hoogdalem MW, Wexelblatt SL, Akinbi HT, Vinks AA, Mizuno T. A review of pregnancy-induced changes in opioid pharmacokinetics, placental transfer, and fetal exposure: towards fetomaternal physiologically-based pharmacokinetic modeling to improve the treatment of neonatal opioid withdrawal syndrome. *Pharmacol Ther*. 2021. <https://doi.org/10.1016/j.pharmthera.2021.108045>.
20. Jones HE, Dengler E, Garrison A, O'Grady KE, Seashore C, Horton E, et al. Neonatal outcomes and their relationship to maternal buprenorphine dose during pregnancy. *Drug Alcohol Depend*. 2014;134:414-7. <https://doi.org/10.1016/j.drugalcdep.2013.11.006>.
21. Dashe JS, Sheffield JS, Olscher DA, Todd SJ, Jackson GL, Wendel GD. Relationship between maternal methadone dosage and neonatal withdrawal. *Obstet Gynecol*. 2002;100:1244-9. [https://doi.org/10.1016/s0029-7844\(02\)02387-6](https://doi.org/10.1016/s0029-7844(02)02387-6).
22. Dryden C, Young D, Hepburn M, Mactier H. Maternal methadone use in pregnancy: factors associated with the development of neonatal abstinence syndrome and implications for healthcare resources. *BJOG*. 2009;116:665-71. <https://doi.org/10.1111/j.1471-0528.2008.02073.x>.
23. Schuh KJ, Johanson CE. Pharmacokinetic comparison of the buprenorphine sublingual liquid and tablet. *Drug Alcohol Depend*. 1999;56:55-60. [https://doi.org/10.1016/s0376-8716\(99\)00012-5](https://doi.org/10.1016/s0376-8716(99)00012-5).
24. Strain EC, Moody DE, Stoller KB, Walsh SL, Bigelow GE. Relative bioavailability of different buprenorphine formulations under chronic dosing conditions. *Drug Alcohol Depend*. 2004;74:37-43. <https://doi.org/10.1016/j.drugalcdep.2003.11.008>.

25. Chawarski MC, Moody DE, Pakes J, O'Connor PG, Schottenfeld RS. Buprenorphine tablet versus liquid: a clinical trial comparing plasma levels, efficacy, and symptoms. *J Subst Abuse Treat.* 2005;29:307-12. <https://doi.org/10.1016/j.jsat.2005.08.011>.
26. Harris DS, Mendelson JE, Lin ET, Upton RA, Jones RT. Pharmacokinetics and subjective effects of sublingual buprenorphine, alone or in combination with naloxone: lack of dose proportionality. *Clin Pharmacokinet.* 2004;43:329-40. <https://doi.org/10.2165/00003088-200443050-00005>.
27. Nath RP, Upton RA, Everhart ET, Cheung P, Shwonek P, Jones RT, et al. Buprenorphine pharmacokinetics: relative bioavailability of sublingual tablet and liquid formulations. *J Clin Pharmacol.* 1999;39:619-23. <https://doi.org/10.1177/00912709922008236>.
28. Dong R, Wang H, Li D, Lang L, Gray F, Liu Y, et al. Pharmacokinetics of sublingual buprenorphine tablets following single and multiple doses in Chinese participants with and without opioid use disorder. *Drugs R D.* 2019;19:255-65. <https://doi.org/10.1007/s40268-019-0277-9>.
29. Ciraulo DA, Hitzemann RJ, Somoza E, Knapp CM, Rotrosen J, Sarid-Segal O, et al. Pharmacokinetics and pharmacodynamics of multiple sublingual buprenorphine tablets in dose-escalation trials. *J Clin Pharmacol.* 2006;46:179-92. <https://doi.org/10.1177/0091270005284192>.
30. Kalluri HV, Zhang H, Caritis SN, Venkataramanan R. A physiologically based pharmacokinetic modelling approach to predict buprenorphine pharmacokinetics following intravenous and sublingual administration. *Br J Clin Pharmacol.* 2017;83:2458-73. <https://doi.org/10.1111/bcp.13368>.
31. Zhang H, Kalluri HV, Bastian JR, Chen H, Alshabi A, Caritis SN, et al. Gestational changes in buprenorphine exposure: A physiologically-based pharmacokinetic analysis. *Br J Clin Pharmacol.* 2018;84:2075-87. <https://doi.org/10.1111/bcp.13642>.
32. Silva LL, Silvola RM, Haas DM, Quinney SK. Physiologically based pharmacokinetic modelling in pregnancy: model reproducibility and external validation. *Br J Clin Pharmacol.* 2021;doi: 10.1111/bcp.15018. <https://doi.org/10.1111/bcp.15018>.
33. Johnson TN, Jamei M, Rowland-Yeo K. How does in vivo biliary elimination of drugs change with age? Evidence from in vitro and clinical data using a systems pharmacology approach. *Drug Metab Dispos.* 2016;44:1090-8. <https://doi.org/10.1124/dmd.115.068643>.
34. NCBI. National Center for Biotechnology Information: PubChem Compound Summary for CID 644073, Buprenorphine. 2022. <<https://pubchem.ncbi.nlm.nih.gov/compound/644073>> Accessed 20 April 2022.
35. Avdeef A, Barrett DA, Shaw PN, Knaggs RD, Davis SS. Octanol-, chloroform-, and propylene glycol dipelargonat-water partitioning of morphine-6-glucuronide and other related opiates. *J Med Chem.* 1996;39:4377-81. <https://doi.org/10.1021/jm960073m>.
36. Bullingham RE, McQuay HJ, Moore A, Bennett MR. Buprenorphine kinetics. *Clin Pharmacol Ther.* 1980;28:667-72. <https://doi.org/10.1038/clpt.1980.219>.
37. Elkader A, Sproule B. Buprenorphine: clinical pharmacokinetics in the treatment of opioid dependence. *Clin Pharmacokinet.* 2005;44:661-80. <https://doi.org/10.2165/00003088-200544070-00001>.
38. Takahashi Y, Ishii S, Arizono H, Nishimura S, Tsuruda K, Saito N, et al. [Pharmacokinetics of buprenorphine hydrochloride (BN\*HCl) (1): absorption, distribution, metabolism and excretion after percutaneous (TSN-09: BN\*HCl containing tape application) or subcutaneous administration of BN\*HCl in rats]. *Xenobiot Metab Dispos.* 2001;16:569-83. <https://doi.org/10.2133/dmpk.16.569>.
39. Hassan HE, Myers AL, Coop A, Eddington ND. Differential involvement of P-glycoprotein (ABCB1) in permeability, tissue distribution, and antinociceptive activity of methadone, buprenorphine, and diprenorphine: in vitro and in vivo evaluation. *J Pharm Sci.* 2009;98:4928-40. <https://doi.org/10.1002/jps.21770>.

40. Holland MJ, Carr KD, Simon EJ. Pharmacokinetics of [3H]-buprenorphine in the rat. *Res Commun Chem Pathol Pharmacol*. 1989;64:3-16.
41. Kuhlman JJ, Jr., Lalani S, Magluilo J, Jr., Levine B, Darwin WD. Human pharmacokinetics of intravenous, sublingual, and buccal buprenorphine. *J Anal Toxicol*. 1996;20:369-78. <https://doi.org/10.1093/jat/20.6.369>.
42. Picard N, Cresteil T, Djebli N, Marquet P. In vitro metabolism study of buprenorphine: evidence for new metabolic pathways. *Drug Metab Dispos*. 2005;33:689-95. <https://doi.org/10.1124/dmd.105.003681>.
43. Chang Y, Moody DE. Glucuronidation of buprenorphine and norbuprenorphine by human liver microsomes and UDP-glucuronosyltransferases. *Drug Metab Lett*. 2009;3:101-7. <https://doi.org/10.2174/187231209788654117>.
44. Cubitt HE, Houston JB, Galetin A. Relative importance of intestinal and hepatic glucuronidation-impact on the prediction of drug clearance. *Pharm Res*. 2009;26:1073-83. <https://doi.org/10.1007/s11095-008-9823-9>.
45. Reckitt & Colman Pharmaceuticals. NDA: 20-733 Suboxone(r) sublingual tablets – Clinical pharmacology/biopharmaceutics review. Richmond, VA: Reckitt & Colman. 2000.
46. Moore JN, Gastonguay MR, Ng CM, Adeniyi-Jones SC, Moody DE, Fang WB, et al. The pharmacokinetics and pharmacodynamics of buprenorphine in neonatal abstinence syndrome. *Clin Pharmacol Ther*. 2018;103:1029-37. <https://doi.org/10.1002/cpt.1064>.
47. Bullingham RE, McQuay HJ, Porter EJ, Allen MC, Moore RA. Sublingual buprenorphine used postoperatively: ten hour plasma drug concentration analysis. *Br J Clin Pharmacol*. 1982;13:665-73. <https://doi.org/10.1111/j.1365-2125.1982.tb01434.x>.
48. Bai SA, Xiang Q, Finn A. Evaluation of the pharmacokinetics of single- and multiple-dose buprenorphine buccal film in healthy volunteers. *Clin Ther*. 2016;38:358-69. <https://doi.org/10.1016/j.clinthera.2015.12.016>.
49. Lim SCB, Schug S, Krishnarajah J. The pharmacokinetics and local tolerability of a novel sublingual formulation of buprenorphine. *Pain Med*. 2019;20:143-52. <https://doi.org/10.1093/pm/pnx321>.
50. Mendelson J, Upton RA, Everhart ET, Jacob P, 3rd, Jones RT. Bioavailability of sublingual buprenorphine. *J Clin Pharmacol*. 1997;37:31-7. <https://doi.org/10.1177/009127009703700106>.
51. Huestis MA, Cone EJ, Pirnay SO, Umbricht A, Preston KL. Intravenous buprenorphine and norbuprenorphine pharmacokinetics in humans. *Drug Alcohol Depend*. 2013;131:258-62. <https://doi.org/10.1016/j.drugalcdep.2012.11.014>.
52. McAleer SD, Mills RJ, Polack T, Hussain T, Rolan PE, Gibbs AD, et al. Pharmacokinetics of high-dose buprenorphine following single administration of sublingual tablet formulations in opioid naive healthy male volunteers under a naltrexone block. *Drug Alcohol Depend*. 2003;72:75-83. [https://doi.org/10.1016/s0376-8716\(03\)00188-1](https://doi.org/10.1016/s0376-8716(03)00188-1).
53. Jonsson M, Mundin G, Sumner M. Pharmacokinetic and pharmaceutical properties of a novel buprenorphine/naloxone sublingual tablet for opioid substitution therapy versus conventional buprenorphine/naloxone sublingual tablet in healthy volunteers. *Eur J Pharm Sci*. 2018;122:125-33. <https://doi.org/10.1016/j.ejps.2018.06.024>.
54. Moody DE, Fang WB, Morrison J, McCance-Katz E. Gender differences in pharmacokinetics of maintenance dosed buprenorphine. *Drug Alcohol Depend*. 2011;118:479-83. <https://doi.org/10.1016/j.drugalcdep.2011.03.024>.

55. Cone EJ, Dickerson SL, Darwin WD, Fudala P, Johnson RE. Elevated drug saliva levels suggest a “depot-like” effect in subjects treated with sublingual buprenorphine. *NIDA Res Monogr.* 1990;105:569.
56. Rodgers T, Rowland M. Physiologically based pharmacokinetic modelling 2: predicting the tissue distribution of acids, very weak bases, neutrals and zwitterions. *J Pharm Sci.* 2006;95:1238-57. <https://doi.org/10.1002/jps.20502>.
57. Yassen A, Olofson E, Romberg R, Sarton E, Teppema L, Danhof M, et al. Mechanism-based PK/PD modeling of the respiratory depressant effect of buprenorphine and fentanyl in healthy volunteers. *Clin Pharmacol Ther.* 2007;81:50-8. <https://doi.org/10.1038/sj.clpt.6100025>.
58. Boom M, Niesters M, Sarton E, Aarts L, Smith TW, Dahan A. Non-analgesic effects of opioids: opioid-induced respiratory depression. *Curr Pharm Des.* 2012;18:5994-6004. <https://doi.org/10.2174/138161212803582469>.
59. Upton RN, Semple TJ, Macintyre PE. Pharmacokinetic optimisation of opioid treatment in acute pain therapy. *Clin Pharmacokinet.* 1997;33:225-44. <https://doi.org/10.2165/00003088-199733030-00005>.